Biogeosciences

# Synergistic effects of $p$CO$_2$ and iron availability on nutrient consumption ratio of the Bering Sea phytoplankton community

**K. Sugie**[1,2], **H. Endo**[3], **K. Suzuki**[2,3], **J. Nishioka**[4], **H. Kiyosawa**[5], **and T. Yoshimura**[1]

[1]Environmental Science Research Laboratory, Central Research Institute of Electric Power Industry, 1646 Abiko, Abiko, Chiba 270-1194, Japan
[2]Faculty of Environmental Earth Science, Hokkaido University and CREST-JST, North 10 West 5, Kita-ku, Sapporo, Hokkaido 060-0810, Japan
[3]Graduate School of Environmental Science, Hokkaido University, North 10 West 5, Kita-ku, Sapporo, Hokkaido 060-0810, Japan
[4]Pan-Okhotsk Research Center, Institute of Low Temperature Science, Hokkaido University, Hokkaido University, North 19 West 8, Kita-ku, Sapporo, Hokkaido 060-0819, Japan
[5]Marine Biological Research Institute of Japan, 4–3–16, Toyomachi, Shinagawa-ku, Tokyo, 142–0042, Japan

*Correspondence to:* K. Sugie (kojisugie@gmail.com)

**Abstract.** Little is known concerning the effect of CO$_2$ on phytoplankton ecophysiological processes under nutrient and trace element-limited conditions, because most CO$_2$ manipulation experiments have been conducted under elements-replete conditions. To investigate the effects of CO$_2$ and iron availability on phytoplankton ecophysiology, we conducted an experiment in September 2009 using a phytoplankton community in the iron limited, high-nutrient, low-chlorophyll (HNLC) region of the Bering Sea basin . Carbonate chemistry was controlled by the bubbling of the several levels of CO$_2$ concentration (180, 380, 600, and 1000 ppm) controlled air, and two iron conditions were established, one with and one without the addition of inorganic iron. We demonstrated that in the iron-limited control conditions, the specific growth rate and the maximum photochemical quantum efficiency ($F_v/F_m$) of photosystem (PS) II decreased with increasing CO$_2$ levels, suggesting a further decrease in iron bioavailability under the high-CO$_2$ conditions. In addition, biogenic silica to particulate nitrogen and biogenic silica to particulate organic carbon ratios increased from 2.65 to 3.75 and 0.39 to 0.50, respectively, with an increase in the CO$_2$ level in the iron-limited controls. By contrast, the specific growth rate, $F_v/F_m$ values and elemental compositions in the iron-added treatments did not change in response to the CO$_2$ variations, indicating that the addition of iron canceled out the effect of the modulation of iron bioavailability due to the change in carbonate chemistry. Our results suggest that high-CO$_2$ conditions can alter the biogeochemical cycling of nutrients through decreasing iron bioavailability in the iron-limited HNLC regions in the future.

## 1 Introduction

The production and elemental composition of marine phytoplankton play a crucial role in driving ocean biogeochemical cycling of nutrients (Redfield et al., 1963). The elemental composition of phytoplankton is affected by changing ambient conditions such as nutrient concentrations and partial pressure of CO$_2$ ($p$CO$_2$) (e.g., Takeda, 1998; Burkhardt et al., 1999; Kudo, 2003), and difference in community compositions (Arrigo et al., 1999; Sugie et al., 2010a). This evidence suggests that the biogeochemical cycling of nutrients could change in response to future global climate change (Hutchins et al., 2009). Therefore, the factors modulating nutrient biogeochemistry are important issues to understand in order to to better predict future environments under climate change. Anthropogenic CO$_2$ emission through burning fossil fuels and land-use change causes an increase in atmospheric CO$_2$ concentrations, which in turn leads to an increase in the

seawater $\mathrm{CO_2}$ level in the global surface ocean (Caldeira and Wickett, 2005). As more anthropogenic $\mathrm{CO_2}$ dissolves into the seawater, the surface ocean acidity will concomitantly increase further, causing ocean acidification (Raven et al., 2005). It has been reported that the ocean acidification affects the elemental composition of phytoplankton, suggesting that oceanic nutrient biogeochemistry will alter according to future high-$\mathrm{CO_2}$ conditions (Hutchins et al., 2009). However, most of the previous studies concerning the effect of $\mathrm{CO_2}$ on phytoplankton ecophysiological processes were conducted under nutrient- and trace element-replete conditions. There is a distinct lack of knowledge regarding the effect of $\mathrm{CO_2}$ on phytoplankton ecophysiology under nutrient- or trace element-limited conditions, despite the fact that the phytoplankton production in oceanic environments is often limited to at least one element such as nitrogen and iron (Saito et al., 2008).

Because iron plays a key role in phytoplankton's metabolic processes such as photosynthesis, respiration, and nitrate and nitrite assimilations (Raven et al., 1999), iron availability also affects the elemental composition of phytoplankton (Takeda, 1998; Sugie et al., 2010a). Phytoplankton productivity, specifically that of diatoms with a relatively large cell size, is limited by iron availability in a large area of the ocean called the high-nutrient, low-chlorophyll (HNLC) region (e.g., de Baar et al., 2005). Recent studies reported that iron availability will change with the increasing contribution of ferrous to ferric iron (Millero et al., 2009) and the conditional stability constant of iron-ligand complex (Shi et al., 2010) in response to the increase in the acidity of seawater. Other human perturbations such as land use and $\mathrm{SO_2}$ and $\mathrm{NO_x}$ emissions will also alter the iron distribution and bioavailability in the open oceans (Mahowald et al., 2009). Therefore, the interactive effects of the ocean acidification and the iron availability are expected to play crucial roles in the biogeochemical cycling of nutrients in the HNLC regions. Previous $\mathrm{CO_2}$ manipulation studies using Southern Ocean and western subarctic Pacific phytoplankton communities suggest that the elemental composition and nutrient drawdown ratio were not affected by $\mathrm{CO_2}$ variations under iron-limited conditions (Feng et al., 2010; Endo et al., 2013). By contrast, the elemental composition of unialgal culture of *Pseudo-nitzschia pseudodelicatissima* changed in response to the change in both $\mathrm{CO_2}$ levels and bioavailable dissolved inorganic iron concentrations (Sugie and Yoshimura, 2013). Further information concerning the interactive effects of iron and ocean acidification on the elemental composition of phytoplankton is still required in order to better understand the future biogeochemistry of nutrients in high-$\mathrm{CO_2}$ oceans.

In the present study, we conducted a $\mathrm{CO_2}$ and iron manipulation study using Bering Sea phytoplankton community. The central Bering Sea basin is one of the ideal ecosystems for investigating the effects of $\mathrm{CO_2}$ and iron because the region is characterized as an iron-limited HNLC region (Leblanc et al., 2005). However, to date, no bioassays for
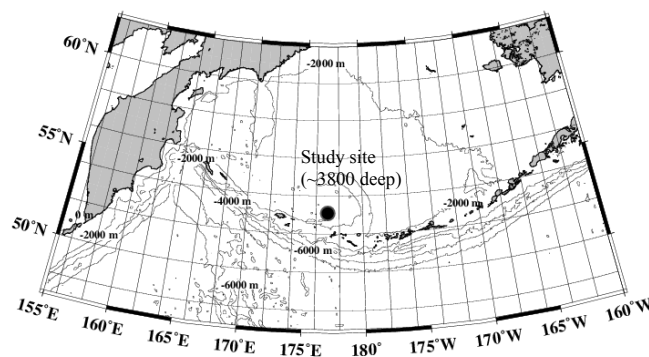


**Fig. 1.** Sampling location ($53°05'$ N, $177°00'$ W) in the Bering Sea basin.

both $\mathrm{CO_2}$ and iron manipulation have been conducted in the region. Here, we demonstrate the effects of $\mathrm{CO_2}$ and iron on the net growth rate, the photochemistry of photosystem (PS) II, the species composition and the elemental composition of phytoplankton. Specifically, we examined these effects on diatoms, which are a key component of carbon and nutrient biogeochemistry, especially in the case of silicon.

## 2   Materials and methods

### 2.1   Sampling location

Seawater for the incubation experiment was collected in the Bering Sea ($53°05'$ N, $177°00'$ W) on 9 September 2009, aboard the RV *Hakuho-Maru* (JAMSTEC) during the KH09-4 cruise (Fig. 1). At the sampling station, surface temperature, salinity, and mixed layer depth were $8.2\,°\mathrm{C}$, $33.10$, and $\sim40\,\mathrm{m}$, respectively. The mixed layer depth was estimated from the first downward increase in $\sigma\text{-}t = 0.02\,\mathrm{m^{-1}}$.

### 2.2   Incubation experiment

Approximately $300\,\mathrm{L}$ of seawater were collected at $10\,\mathrm{m}$ depth using acid-cleaned, Teflon-coated $10\,\mathrm{L}$ Niskin-X sampling bottles (General Oceanics) attached to a CTD-CMS. Seawater for the experiment was sieved through a $197\,\mu\mathrm{m}$ acid-cleaned Teflon-mesh to eliminate mesozooplankton, and the pre-screened seawater was poured into six acid-washed $50\,\mathrm{L}$ polypropylene tanks to homogenize seawater samples. The two tanks were used for Fe-limited conditions (controls). Inorganic iron stock solution was added to four tanks to make the final concentration of $5\,\mathrm{nmol\,L^{-1}}$ (Fe-added treatments), and then the seawater samples were mixed thoroughly but gently. Then the seawater was dispensed into three identical $12\,\mathrm{L}$ polycarbonate incubation bottles per $50\,\mathrm{L}$ tank. Carbonate chemistry was manipulated by injecting $\mathrm{CO_2}$ concentration ($x\mathrm{CO_2}$) controlled dry-air (Nissan Tanaka Corp., Saitama, Japan) directly into the incubation bottles at a flow rate of $100\,\mathrm{mL}$ per minute for the first 24 h. Thereafter,

the flow rate was maintained at 50 mL per minute during the culture experiment (Yoshimura et al., 2010). The $x$CO$_2$ of the injected air was set at 380 and 600 ppm for the controls (hereafter C-380 and C-600, respectively) and 180, 380, 600, and 1000 ppm for the Fe-added treatments (hereafter Fe-180, Fe-380, Fe-600, and Fe-1000, respectively). The air injected into all of the bottles was passed through a 0.2 μm in-line filter to avoid trace element contaminations from gas cylinders and lines. The dissolved inorganic carbon (DIC) and total alkalinity (TA) were measured periodically to calculate carbonate chemistry (see below). Incubations lasted for 7 days in an on-deck incubator. The temperature of the incubator was maintained at near-ambient sea surface temperature ($\sim$ 8°C) by a constant temperature water circulator (Yamato Scientific Co., Ltd.). The incubator was covered with neutral density mesh to decrease surface irradiance by 50 %. Photon flux was measured using a $4\pi$ quantum sensor in combination with a data logger (JFE Advantech Co., Ltd.). Sampling for size-fractionated (10 μm and GF/F) Chlorophyll $a$ (Chl $a$)and nutrients was carried out daily. Similarly, samples for particulate organic carbon (POC), particulate nitrogen (PN), biogenic silica (BSi), DIC, TA, microscopic observation, and the maximum photochemical quantum yield ($F_{\mathrm{v}}/F_{/}m$) of PS II for phytoplankton were collected at days 1.9, 3.6, 5, and 5.7 for the Fe-limited controls (hereafter day 2, 4, and 6, respectively) and at days 1.9, 2.6, 4.7, and 6.6 for the Fe-added treatments (hereafter day 2, 3, 5, and 7, respectively). Samples to test for total dissolvable iron (TD-Fe, unfiltered) and dissolved iron (D-Fe, < 0.22 m) at the beginning of the experiment were collected directly from the spigot of the Niskin-X sampling bottles, using a 0.22 μm cartridge filter (Merck Millipore) with gravity filtration for D-Fe. At the end of the experiment, TD-Fe samples were collected from the incubation bottles. Size-fractionated Chl $a$ samples were collected sequentially on the 10 μm pore size of polycarbonate filter (Whatman) without vacuum and on GF/F filter (Whatman) under gentle vacuum at < 100 mm Hg. Filter samples for Chl $a$ were extracted with $N$, $N$-dimethylformamide immediately after the filtration and stored at −20 °C in the dark at least 24 h until aboard analysis (Suzuki and Ishimaru, 1990). Samples of POC and PN were collected on a precombusted (450 °C, 4 h) GF/F filter. Samples of BSi were collected on the 0.4 μm pore size of polycarbonate membrane filter under gentle vacuum. Samples of POC, PN, BSi, and nutrients were stored at −20 °C until analysis in an onshore laboratory. The DIC and TA samples were collected into gastight glass vials and poisoned with HgCl$_2$ prior to the storage at 4 °C for onshore analysis. For microscopic analysis, Lugol's acidic iodine solution was added to seawater (4 % final volume). For iron analysis, seawater samples were acidified at pH 3.2 with 10 mol L$^{-1}$ formic acid and 2.4 mol L$^{-1}$ ammonium formate buffer after the sample collection and stored at room temperature for several months until analysis. To examine the silicification of the diatom cells, we conducted incubations using 2-(4-pyridyl)-5-((4-(2-dimethylaminoethyl-aminocarbamoyl)-methoxy)phenyl)oxazole (PDMPO) fluorescence probe (Life Technologies Corp.), which incorporates and stains newly deposited diatom frustules during their growth (Leblanc and Hutchins, 2005; Ichinomiya et al., 2010). We used the fluorescence intensity of the PDMPO within the frustule as an index of silification of the diatom cells under different CO$_2$ and iron conditions. Seawater samples for PDMPO labeling incubation were collected from the 12 L polycarbonate incubation bottles by siphon and dispensed into acid-cleaned 170 mL polycarbonate bottles without head space. Triplicate 170 mL incubation bottles were prepared for each treatment. The PDMPO incubation was started on day 3.3 of the Fe-limited control treatments and day 2.3 of the Fe-added treatments, when macronutrients were not exhausted. The PDMPO stock solution (1 mmol L$^{-1}$) was added to the 170 mL incubation bottles to make 0.25 μmol L$^{-1}$ (Leblanc and Hutchins, 2005). The bottles were incubated for 24 h in the onboard incubator. After the incubation, seawater samples were filtered onto black-stained 0.4 μm polycarbonate filters and mounted on a glass slide with immersion oil. The glass slide was stored at −20 °C until onshore microscopic observation and digital image analysis was carried out. Chl $a$ samples were collected on GF/F filter at the end of the PDMPO incubations to compare the growth of phytoplankton between the 170 mL and 12 L incubation bottles. Unfortunately, we were not able to measure carbonate chemistry during the PDMPO experiment due to a water volume limitation. However, the relatively low biomass together with the short incubation time allows us to assume that the change in the carbonate chemistry of the bottles during the incubation period was small.

## 2.3 Chemical and biological analyses

Chl $a$ concentration was measured with the Turner Design 10-AU fluorometer (Welschmeyer, 1994). The net specific growth rate of phytoplankton was calculated from the linear regression between the time (day) and the natural log of Chl $a$ concentrations, using the data gathered before nutrient depletions. The nutrients were measured using a QuAAtro-2 continuous flow analyzer (Bran+Luebbe, SPX Corp.), and iron concentrations were measured by flow-injection method with chemiluminescence detection (Obata et al., 1993). Our iron-measurement method was carefully assessed using the Sampling and Analysis of Fe (SAFe) cruise reference standard seawater for an inter-comparison study distributed by the Moss Landing Marine Laboratory and University of California Santa Cruz. According to this method, we measured $0.10 \pm 0.010$ nmol L$^{-1}$ ($n = 3$) and $0.99 \pm 0.023$ nmol L$^{-1}$ ($n = 3$) D-Fe for concentrations of $0.094 \pm 0.008$ nmol L$^{-1}$ ($S$) and $0.923 \pm 0.029$ nmol L$^{-1}$ (D2) D-Fe (www.geotraces.org), respectively for the reference standard seawater. Filter samples for POC- and PN-analysis were freeze-dried and then exposed to HCl fumes overnight to remove inorganic carbon; these concentrations

were then measured by a CHN analyzer (Perkin Elmer Inc.). For BSi analysis, the filter sample was digested by heating to 85 °C for 2 h in a 0.5 % Na$_2$CO$_3$ solution (Paasche, 1980). After being neutralized with 0.5 mol L$^{-1}$ HCl, the silicic acid concentration was measured using a QuAAtro-2 continuous flow analyzer. All data for POC, PN, and BSi concentrations were corrected by subtracting appropriate filter blanks. The elemental compositions (POC:PN (hereafter C:N), BSi:PN (Si:N), BSi:POC (Si:C)) of phytoplankton produced during the experiment were calculated by subtracting the value at the beginning of the experiment from the value on the day before nutrient depletions. DIC and TA were measured by the potentiometric Gran plot method with dilute HCl (0.1000 mol L$^{-1}$; Wako Co. Ltd.) using a total alkalinity analyzer (Kimoto Electric Co., Ltd.) according to the method of Edmond (1970). The stability of the titration analysis was checked by DIC reference material (KANSO Co., Ltd., Osaka, Japan), whereby the DIC value was traceable to the certified reference material supplied by Andrew Dickson at University of California, San Diego. The analytical errors were < 0.1 % for both DIC ($\sim$ 1.1 μmol kg$^{-1}$) and TA ($\sim$ 1.4 μmol kg$^{-1}$). pH (total scale) and $p$CO$_2$ values were calculated from DIC and TA data using the CO2SYS program (Lewis and Wallance, 1998). For microscopic analysis, an adequate volume of fixed seawater was poured into a settling chamber and was allowed to settle for at least 24 h before identification using a phase contrast inverted microscope (Hasle, 1978). Diatom species were identified according to Hasle and Syvertsen (1997). Cell volume of the dominant diatom species was measured as described by Hillebrand et al. (1999), and the cell volume was converted to carbon biomass as reported by Menden-Deuer and Lessard (2000). For $F_v/F_m$ measurement, seawater samples were stored for 15 min in a bench-top incubator at 8 °C in the dark. $F_v/F_m$ values were measured with the Fluorescence Induction and Relaxation (FIRe) system (Satlantic Inc.), in which a blue (455 nm with 60 nm bandwidth) light-emitted diode was incorporated for excitation. The FIRe protocol involved single-turnover flashes within 80 μs duration. Triplicate samples were measured with 10 iterations per sample. The background fluorescence was also measured and subtracted from the sample values using 0.2 μm filtered seawater (Gorbunov and Falkowski, 2004). Raw data were collected following the protocol of the Fireworx program for MATLAB software, developed by Audrey B. Barnett (Dalhousie University), and processed with this software in order to obtain $F_v/F_m$ values. The PDMPO-stained samples were observed by epifluorescence microscope (Olympus Corp.), and the picture was taken by digital camera (Olympus Corp.). The fluorescence intensity of PDMPO-stained diatom frustule was analyzed using digital images with Image-Pro Plus software (Media Cybernetics Inc.). To minimize the differences in cell size among the different diatom species and among the different treatments, cellular fluorescence intensity was normalized to the area of the fluorescent frustules. During the epifluores-
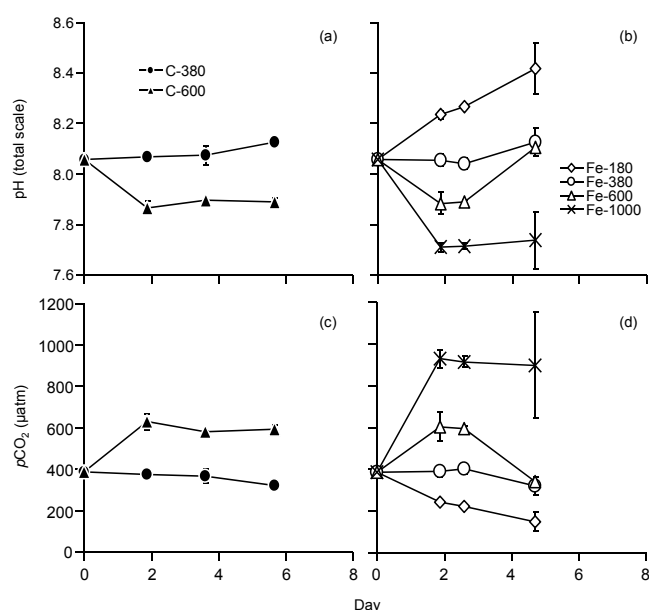


**Fig. 2.** Temporal change in **(a)** and **(b)** pH (total scale) and **(c)** and **(d)** $p$CO$_2$ during the course of incubation experiment. **(a)** and **(c)**: controls. **(b)** and **(d)**: iron added treatments. Data represent mean $\pm$ 1SD of the three bottles.

cence microscope observation, we used a 6 % Neutral Density (ND) filter to minimize the decay of fluorescence, and the ND filter was removed only when taking pictures.

## 3  Results

### 3.1  Experimental conditions

At the beginning of the experiment, the nutrient concentrations were 18.1 ± 0.1 μmol L$^{-1}$ NO$_3^-$ + NO$_2^-$, 0.64 ± 0.2 μmol L$^{-1}$ NH$_4^+$, 1.47 ± 0.01 μmol L$^{-1}$ PO$_4^{3-}$, and 17.0 ± 0.1 μmol L$^{-1}$ Si(OH)$_4$ (mean ± 1SD, $n = 6$). The D-Fe and TD-Fe concentrations of the seawater sample were 0.17 and 1.35 nmol L$^{-1}$, respectively. The TA, DIC, pH, and $p$CO$_2$ of the seawater sample at the beginning of the experiment were 2249 ± 3.5 μmol kg$^{-1}$, 2086 ± 1.6 μmol L$^{-1}$, 8.06 ± 0.01, and 386 ± 11 μatm, respectively (mean ± 1SD, $n = 4$). Mean daily photon flux density in the on-deck incubator was 8.7 ± 3.2 mol photon m$^{-2}$ day$^{-1}$ during the 7 days of the experiment, ranging from 4.9 to 13.0 mol photon m$^{-2}$ day$^{-1}$.

During the course of the experiment, manipulation of carbonate chemistry was successfully archived within the first 2 days by the $x$CO$_2$-controlled air bubbling, but the conditions in the Fe-added treatments were gradually changed with incubation time (Fig. 2). During the 2- to 6-day period, the mean pH in the C-380 treatment was 8.09 ± 0.03, the mean pH in the C-380 and C-600 treatments were 8.09 ± 0.03 and 7.88 ± 0.02, respectively. Mean

$p$CO$_2$ in the C-380 and C-600 treatments were $356 \pm 28$ and $602 \pm 25$ µatm, respectively. In the Fe-added treatment, the increase in pH and the decrease in $p$CO$_2$ were observed in all CO$_2$ manipulation treatments due to the intensive phytoplankton production in the bottles (Fig. 2b, d). At the end of the incubations, TD-Fe concentrations in the C-380, C-600, Fe-180, Fe-380, Fe-600, and Fe-1000 media were $0.27 \pm 0.02$, $0.29 \pm 0.04$, $4.60 \pm 0.16$, $4.48 \pm 0.10$, $4.34 \pm 0.06$, and $4.18 \pm 0.20$ nmol L$^{-1}$, respectively (mean $\pm 1$SD of the three incubation bottles), and the concentrations did not differ significantly between the C-380 and C-600 treatments or among the Fe-added treatments. Therefore, we successfully conducted the experiments without inadvertent iron contaminations in the control treatments and Fe-added treatments.

## 3.2 Phytoplankton growth

In the control conditions, net specific growth rate of both size fractions was significantly higher in the C-380 treatment ($> 10$ µm: $0.31 \pm 0.02$ d$^{-1}$ (mean $\pm 95\%$ CL of regression), GF/F–10 µm: $0.13 \pm 0.03$ d$^{-1}$) than in the C-600 treatment ($> 10$ µm: $0.28 \pm 0.03$ d$^{-1}$, GF/F–10 µm: $0.06 \pm 0.01$ d$^{-1}$) ($> 10$ µm: $p = 0.011$, GF/F–10 µm: $p = 0.047$; ANOVA) (Fig. 3a, c). Net specific growth rate was higher in the Fe-added treatments than that in the controls, without statistically significant difference in the CO$_2$ levels, which ranged from $0.82 \pm 0.05$ to $0.92 \pm 0.04$ d$^{-1}$ for the $> 10$ µm fraction and $0.43 \pm 0.03$ to $0.52 \pm 0.03$ d$^{-1}$ for the GF/F–10 µm fraction (Fig. 3b, d). The total Chl $a$ concentrations in the Fe-600 and Fe-1000 treatments on day 5 were lower relative to the Fe-180 and Fe-380 treatments (Fig. 3f), although the difference was not affected significantly on the net specific growth rate. These trends in total Chl $a$ concentrations were almost identical to that of the large fraction of Chl $a$ because of the high dominance ($> \sim 90\%$) of the large-sized Chl $a$ (Fig. 3e, f). At the beginning of the experiment, the concentrations of POC, PN, and BSi were 10, 1.5, and 3.8 µmol L$^{-1}$, respectively. On day 6, POC concentrations increased to 40.1 and 23.8 µmol L$^{-1}$ in the C-380 and C-600 treatments, respectively. In the Fe-added treatments, POC concentration increased to 66–89 µmol L$^{-1}$ on day 5 without statistically significant difference between the CO$_2$ variations, and it increased further after the nutrient depletions (Supplement Fig. 1). Net specific growth rate calculated from the POC data showed the same trend as estimated from Chl $a$. The increase in PN and BSi was closely followed by the amount of nutrient drawdown described below (Supplement Fig. 1).

The $F_v/F_m$ in the controls decreased with incubation time, and on days 2 and 4 the values in the C-600 treatment were significantly lower than those in the C-380 treatment (day 2: $p < 0.01$; day 4: $p = 0.012$, ANOVA) (Fig. 4a). In the Fe-added treatments, the $F_v/F_m$ values increased from 0.35 (day 0) to $\sim 0.55$ during the first 3 days, followed by a slight de-
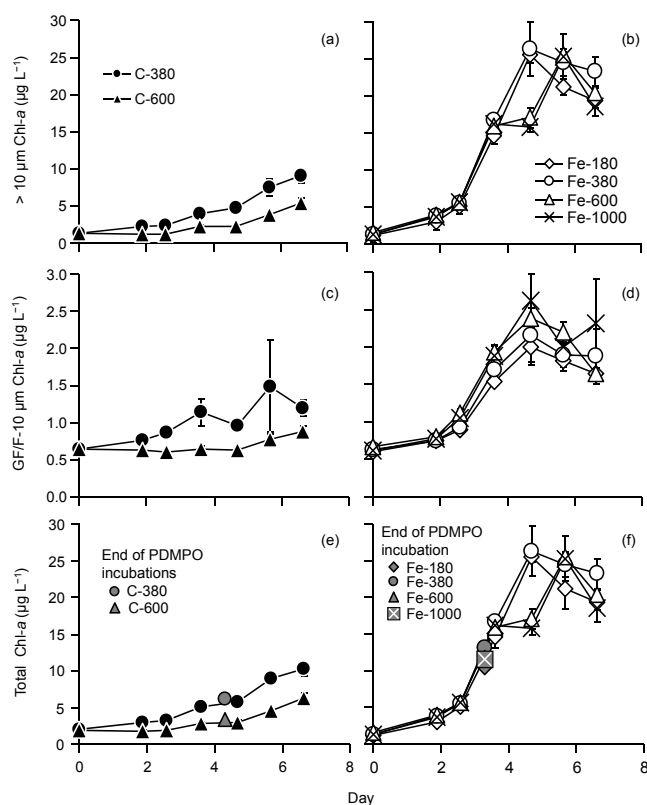


**Fig. 3.** Temporal change in size-fractionated chlorophyll $a$ concentrations. **(a)** and **(b)**: $> 10$ µm, **(c)** and **(d)**: 10 µm–GF/F ($\sim 0.7$ µm), and **(e)** and **(f)**: total concentrations. Left column: controls, right column: iron added treatments. Data represent mean $\pm 1$SD of the three bottles.

crease with time; there were no statistically significant variations between the CO$_2$ treatments (Fig. 4b).

At the beginning of the incubation, a microscopically identifiable phytoplankton community in the bottles was dominated by diatoms followed by dinoflagellates (Fig. 5). *Chaetoceros* subgenus *Hyalochaete* spp. prominently increased during the first 2–3 days and represented $\sim 70\%$ of the carbon biomass of the phytoplankton community in all treatments (Fig. 5). Among the *Hyalochaete* spp., *C. compressus/contortus* complex and *C. constrictus* were the dominant species, followed by *C. diadema*, *C. brevis/laciniosus* complex, *C. debilis*, *C. radicans*, *C. teres*, *C. curvisetus* and *C. socialis*. After the peak of the *Hyalochaete* spp., *Pseudonitzschia* spp. and other centric diatoms such as *Eucampia groenlandica* increased in the controls (Fig. 5a, b). In the Fe-added conditions, *Pseudo-nitzschia* spp., *Chaetoceros* subgenus *Phaeoceros* spp. and Rhizosoleniaceae such as *Rhizosolenia* spp., *Proboscia alata*, and *Dactyliosolen fragilissimus* increased in the lower two CO$_2$ treatments after day 4 (Fig. 5c, d). By contrast, Rhizosoleniaceae did not increase in dominancy after day 4 in the higher two CO$_2$ treatments (Fig. 5e, f). Note that most *Hyalochaete* spp. can form resting
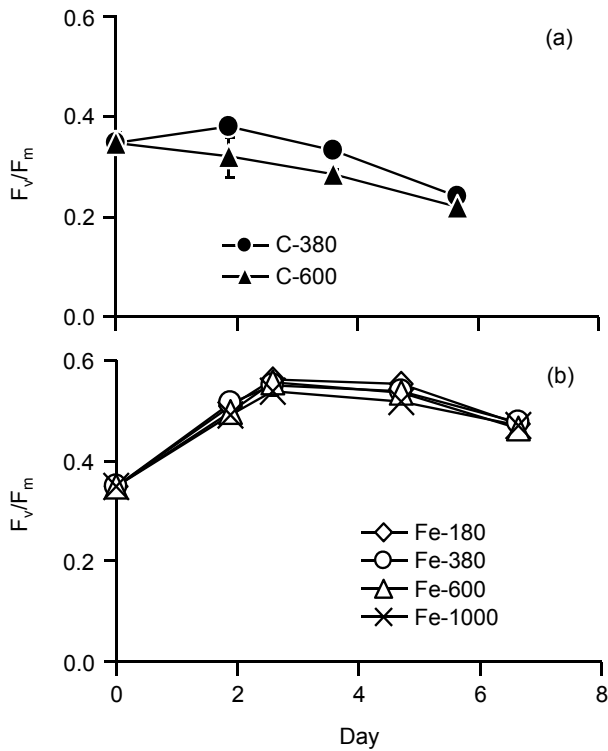
**Fig. 4.** Temporal change in $F_\text{v}/F_\text{m}$ values. **(a)** controls and **(b)** iron added treatments.

spores and are considered coastal species (Hasle and Syvertsen, 1997; Sugie et al., 2010a), although no resting spores were observed during the experiment.

### 3.3 Nutrient dynamics

In the controls, measurable amounts of the nutrients remained at the end of incubations; the one exception was that Si(OH)4 was below detection limit ($\sim$0.2 µmol $\text{L}^{-1}$) in the C-380 treatment on day 7 (Fig. 6a, c, e, g). The $\text{NO}_3^- + \text{NO}_2^-$, $\text{PO}_4^{3-}$, and Si(OH)$_4$ drawdowns were smaller in the C-600 treatment than in the C-380 treatment, which reflects the Chl $a$ dynamics (Fig. 3). In the Fe-added treatments, nutrients were exhausted between days 4 and 6 in all $\text{CO}_2$ conditions (Fig. 6b, d, f); the one exception was $\text{NH}_4^+$, which was detectable ($\sim$0.1 µmol $\text{L}^{-1}$) at the end of the incubations (Fig. 6h). We calculated nutrient drawdown per unit Chl $a$ increase before nutrient depletions as an index of nutrient requirement per unit phytoplankton biomass (Fig. 7). The ($\text{NO}_3^- + \text{NO}_2^-$)/Chl $a$ in the C-380 treatment was significantly higher than that in the C-600 treatment, whereas no significant change was observed among $\text{CO}_2$ variations in the Fe-added treatments ($p < 0.01$, Dunnett's $t$ test). In the Fe-added treatment, $\text{PO}_4^{3-}$/Chl $a$ and Si(OH)$_4$/Chl $a$ showed a similar trend to that of ($\text{NO}_3^- + \text{NO}_2^-$)/Chl $a$, in that no significant change was detected due to $\text{CO}_2$ variations. The nutrient drawdown per unit Chl $a$ in the controls was higher
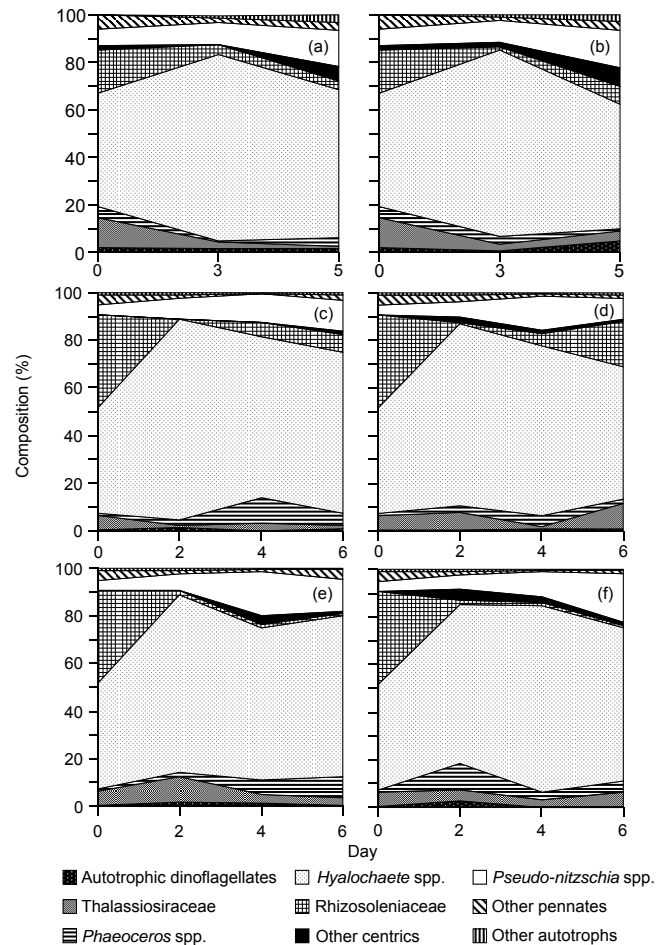


**Fig. 5.** Temporal change in the species composition of diatoms and other autotrophs in terms of carbon biomass. **(a)** 380 ppm $\text{CO}_2$ control, **(b)** 600 ppm $\text{CO}_2$ control, **(c)** 180 ppm $\text{CO}_2$ Fe added, **(d)** 380 ppm $\text{CO}_2$ Fe added, **(e)** 600 ppm Fe added and **(f)** 1000 ppm $\text{CO}_2$ Fe added treatments.

than that in the Fe-added treatments ($p < 0.01$, Dunnett's $t$ test), probably due to an increase in the Chl $a$ quota of phytoplankton in the Fe-added treatments (Raven, et al., 1999; Sugie et al., 2011).

### 3.4 PDMPO fluorescence of the frustule

The Chl $a$ concentrations at the end of the PDMPO incubation closely matched those in the 12 L incubation bottles, suggesting the environmental conditions, especially iron availability, were unaltered after being dispensed into into the 170 mL of PDMPO-incubation bottles (Fig. 3e, f). In the control conditions, the fluorescence intensity of the PDMPO in the frustule did not change between C-380 and C-600 treatment except for *Fragilariopsis* spp., which showed 14 % decrease of the fluorescence with increasing $\text{CO}_2$ levels (Fig. 8, Supplement). In the Fe-added treatments, we did not measure consistent $\text{CO}_2$-dependent trends in the PDMPO

fluorescence, but the values in *C. brevis/laciniosus* complex, *C. debilis*, *Pseudo-nitzschia* spp., and *Fragilariopsis* spp. showed decreasing trends with increasing $\mathrm{CO_2}$ concentrations (Fig. 8). The fluorescence values of *Neodenticula seminae* were about two times higher than those of the other species, but no consistent trends against $\mathrm{CO_2}$ variations and iron additions were detected. In general, change in the fluorescence intensities among all treated conditions for the dominant species was small (several percent), but the value of a few minor dominant species changed by 16 % (*C. brevis/laciniosus* complex and *C. debilis*) and $\sim 25$ % (*Pseudo-nitzschia* spp. and *Fragilariopsis* spp.) (Fig. 5).

## 3.5 Elemental compositions

To calculate elemental composition, we subtracted the values of particulate matter concentrations from day 5 to day 0 for Fe-limited controls and from day 4 to day 0 for Fe-added treatments, when the nutrients were not exhausted (Fig. 6). The C : N did not change significantly due to the $\mathrm{CO_2}$ variations and iron additions (Fig. 9a). The Si : N in the Fe-limited controls increased 40 % in response to an increase in the $\mathrm{CO_2}$ level, whereas the ratio did not change due to the $\mathrm{CO_2}$ variations in the Fe-added treatments (Fig. 9b). Similarly, the Si : C increased significantly in the C-600 treatment compared to in the C-380 treatment, and did not show a significant variation in the Fe-added treatments (Fig. 9c). The Si : N and Si : C ratios decreased due to the addition of iron (Fig. 9b, c). The nutrient drawdown ratio of $\mathrm{Si(OH)_4 : (NO_3^- + NO_2^-)}$ showed the same trend as observed in the elemental composition of particulate matter (data not shown). The $\mathrm{(NO_3^- + NO_2^-) : PO_4^{3-}}$ drawdown ratio showed a significant increase in the Fe-added treatments compared to the controls. In the controls, the $\mathrm{(NO_3^- + NO_2^-) : PO_4^{3-}}$ drawdown ratio in the C-600 treatment (12.0 $\pm$ 0.3 mol : mol) was smaller than that in the C-380 treatment (13.5 $\pm$ 0.2 mol : mol), whereas the values did not change due to $\mathrm{CO_2}$ variations in the Fe-added treatments (16.3–16.8 mol : mol).

## 4 Discussion

We observed relatively high Chl *a* ($\sim 2\,\mu\mathrm{g\,L^{-1}}$) with the dominance of coastal, resting spore-forming diatom species throughout the course of the experiment. The temperature, mixed layer depth, and macronutrient concentrations we measured were similar to those reported previously (Fujishima et al., 2001; Leblanc et al., 2005; Onodera and Takahashi, 2009). Karohji (1972) and Martin and Tortell (2006) found that coastal centric diatom species were a dominant diatom group in the eastern Bering Sea shelf, whereas pennate diatoms and oceanic centric diatoms such as *Phaeoceros* spp. could be found around the central Bering Sea basin. The values for dissolved Fe (D-Fe: $< 0.2\,\mu\mathrm{m}$) concentrations in the present study were intermediate in relation to the values
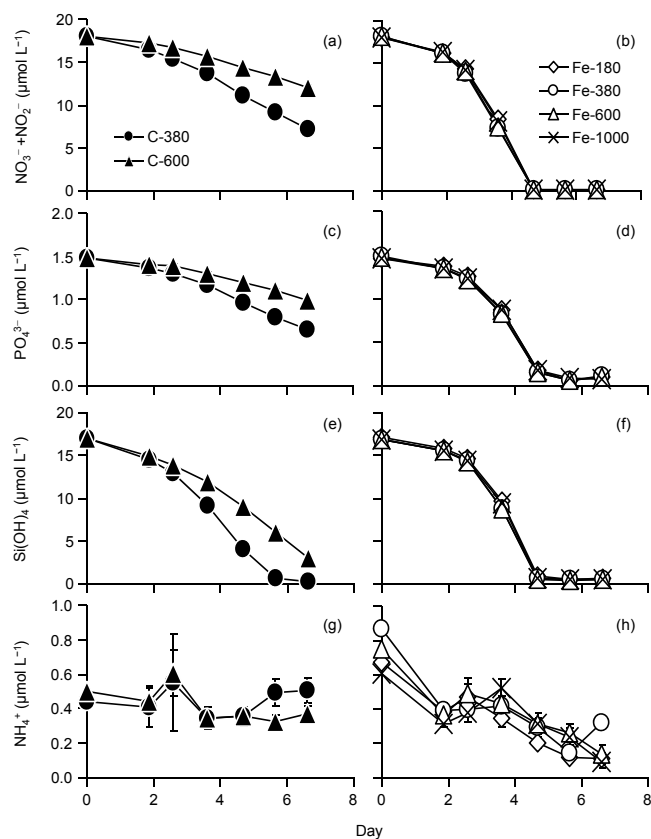


**Fig. 6.** Temporal change in **(a)** and **(b)** $\mathrm{NO_3^- + NO_2^-}$, **(c)** and **(d)** $\mathrm{PO_4^{3-}}$, **(e)** and **(f)** $\mathrm{Si(OH)_4}$, and **(g)** and **(h)** $\mathrm{NH_4^+}$ concentrations. Left column: controls, right column: iron added treatments. Data represent mean $\pm$ 1SD of the three bottles.

measured in the Bering Sea basin in previous studies (0.3–0.78 $\mathrm{nmol\,L^{-1}}$: Fujishima et al., 2001; 0.04–0.10 $\mathrm{nmol\,L^{-1}}$: Leblanc et al., 2005; 0.1–0.3 $\mathrm{nmol\,L^{-1}}$: Takata et al., 2005; 0.01 $\mathrm{nmol\,L^{-1}}$: Buck and Bruland, 2007). By contrast, the total dissolvable iron (TD-Fe, unfiltered) concentrations at the beginning of this study (1.35 $\mathrm{nmol\,L^{-1}}$) were higher than previously reported values ($\leq 0.4\,\mathrm{nmol\,L^{-1}}$: Suzuki et al., 2002; Takata et al., 2005). In general, TD-Fe concentrations were higher in the coastal region compared to the oceanic region (e.g., Johnson et al., 1999). The presence of coastal diatom species with high TD-Fe concentrations indicates a recent intrusion of the coastal seawater mass before the experiment, probably coming from the Aleutian trenches (Mordy et al., 2005; Stabeno et al., 2005). Such a Fe-limited ecosystem with coastal phytoplankton species can often be seen around coastal to oceanic boundaries, such as in the subarctic North Pacific (Sugie et al., 2010a, b). In the Bering Sea basin, the resting spores of the *Hyalochaete* spp. were frequently observed as dominant phytoplankton groups in the mooring sediment trap, close to the site of our experiment (53.5° N, 177° W; Takahashi et al., 2002). However, there have been no reports concerning the effects of $\mathrm{CO_2}$ and iron
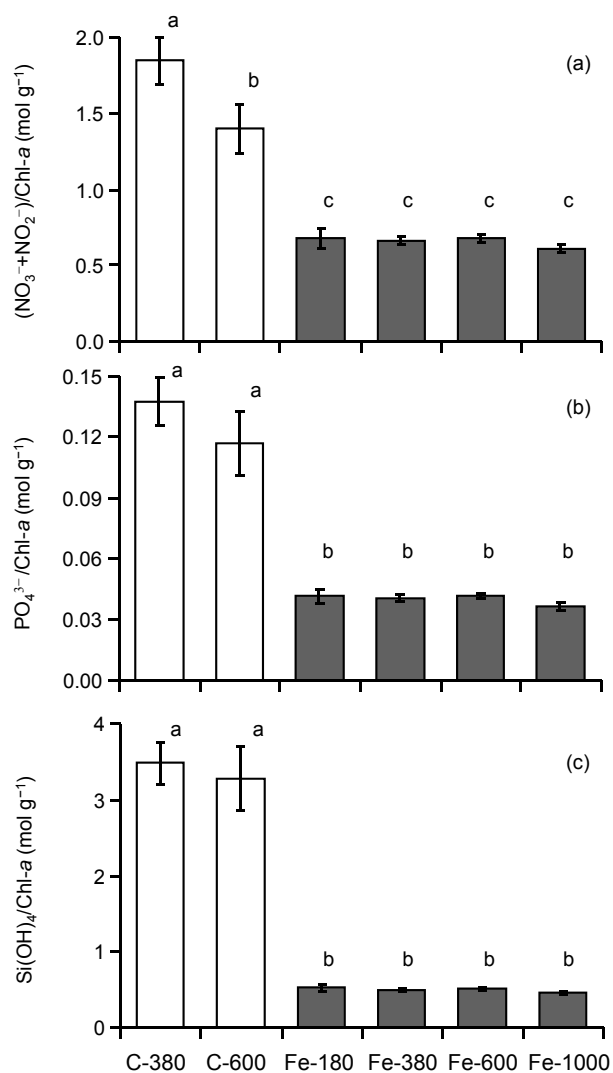
**Fig. 7.** Comparison of nutrient drawdown per unit chlorophyll $a$ (Chl $a$) increase. **(a)** (NO$_3^-$ +NO$_2^-$)/Chl $a$, **(b)** PO$_4^{3-}$/Chl $a$, and **(c)** Si(OH)$_4$/Chl $a$. Data represent mean $\pm$ 1SD of the three bottles. Alphabets above the bar represent statistical result of Tukey's B group test.

on a Fe-limited phytoplankton community with the dominance of coastal diatom species.

## 4.1 Synergistic effects of CO$_2$ and iron on phytoplankton dynamics

The addition of iron stimulates the net specific growth rate and increases $F_v/F_m$ values, indicating that the phytoplankton community in the control conditions was Fe-limited. Suzuki et al. (2002) also observed low $F_v/F_m$ values with low TD-Fe concentrations in the Bering Sea basin during early summer 1999. It is known that iron or nitrogen limitations lead to a decrease in $F_v/F_m$ (e.g., Greene et al., 1992; Suzuki et al., 2002). Furthermore, in the Fe-limited control condi-

tions, significantly higher specific growth rate and $F_v/F_m$ values of phytoplankton in the C-380 compared to those in the C-600 treatment indicate that the phytoplankton community in the C-600 treatment was more severely iron-limited than that in the C-380 treatment. Note that the TD-Fe concentrations did not show a significant change between the two control treatments at the end of the incubations. A recent study reported that iron bioavailability decreases with decreasing pH in seawater by increasing the conditional stability constant of natural iron-ligand complex (Shi et al., 2010); this strongly supports our observations in the control treatments. In addition, the changes in the net specific growth rate and $F_v/F_m$ values in the controls were observed soon after the change in carbonate chemistry. Such a rapid response to the environmental conditions suggests that the principal effect is caused by the change in iron bioavailability of the seawater medium rather than by physiological acclimation of phytoplankton (Xu et al., 2012).

In the Fe-added treatments, we found insignificant difference in net specific growth rate in terms of Chl $a$ and $F_v/F_m$ values among the different CO$_2$ levels. Previous studies have reported that the net growth rates of some phytoplankton species were influenced by the change in CO$_2$ levels, whereas the net growth rate of the phytoplankton community in terms of Chl $a$ was rarely affected due to CO$_2$ variations under iron-replete conditions (Kim et al., 2006; Feng et al., 2009, 2010). In addition, Hopkinson et al. (2010) and Endo et al. (2013) reported that $F_v/F_m$ values did not show a significant difference due to variations in CO$_2$ levels under iron-replete conditions as observed in the present study. This indicates that the photochemistry of PS II is little-affected by CO$_2$ availability under iron-replete conditions. We suggest that the large input of dissolved inorganic iron may cancel out the effect of the modification of iron bioavailability due to the CO$_2$ variations in the Fe-added treatments. Therefore, the effect of CO$_2$ on the phytoplankton dynamics was small during their exponential growth phase under iron-replete conditions.

However, we found that the phytoplankton community of the less dominant species changed slightly with the change in the CO$_2$ levels in the Fe-added treatments after day 4 when the nutrients were exhausted (Fig. 5). By contrast, in the Fe-limited control conditions, phytoplankton community composition did not change due to the CO$_2$ variations. Martin and Tortell (2006) and Hopkinson et al. (2010) reported that the phytoplankton community composition did not change due to CO$_2$ variations under nutrient-replete conditions. The possible difference in the results of the studies may be derived from nutrient conditions. In the present study, the phytoplankton community in the Fe-added treatments also did not change in response to the CO$_2$ variations before nutrient depletions as reported previously (Martin and Tortell, 2006; Hopkinson et al., 2010). Although the effect of increasing CO$_2$ levels on the growth rate of phytoplankton is beneficial for some phytoplankton species (e.g., Kim et al., 2006; Hutchins et al., 2009), the net specific growth rate of
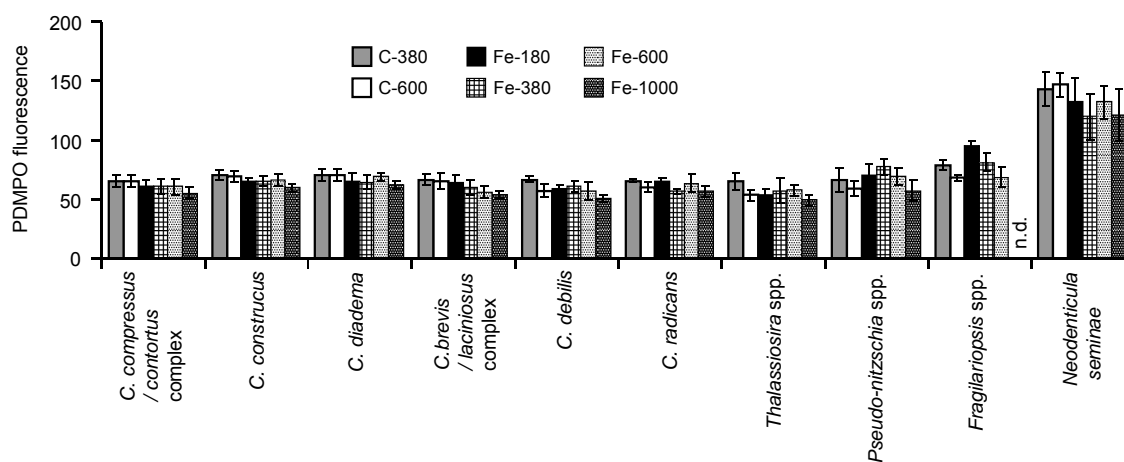
**Fig. 8.** Fluorescence intensity of the PDMPO-stained frustule of the diatom species. n.d.: not detected. Statistical results are shown in Appendix tables.

the diatoms observed before nutrient depletion in the present study may not be influenced in response to the change in CO$_2$ levels. Therefore, we conclude that the increase in CO$_2$ level affects the species composition of phytoplankton under Fe-replete but nutrient depleted conditions.

## 4.2 Synergistic effects of CO$_2$ and iron on the elemental composition of plankton communities

This study demonstrated for the first time that the Si : N and Si : C ratios of a Fe-limited phytoplankton community increase significantly with an increase in CO$_2$ levels. Possible mechanisms underlying the increase in Si : N and Si : C ratios of the diatoms are the increase in silification, the decrease in cellular N and C content of the diatoms due to decreasing iron, nitrate and light availability (Takeda, 1998; Saito and Tsuda, 2003; Marchetti and Harrison, 2007; Sugie et al., 2010a), and ambient high Si(OH)$_4$ concentration or a high Si(OH)$_4$ to NO$_3^-$ ratio (Kudo, 2003; Finkel et al., 2010). In the present study, light conditions were the same in all treatments and the species composition of the diatoms were quite similar in the two control conditions. The ambient Si(OH)$_4$ to NO$_3^-$ ratio was lower in the C-600 treatment than in the C-380 treatment because of the higher Si : N ratio of the particles in the C-600 treatment than in the C-380 treatment. According to the result of PDMPO incubations and Si(OH)$_4$/Chl $a$ values, the silicon content of the diatom frustules of the dominant species was not markedly changed in response to different experimental conditions. The data of (NO$_3^-$ + NO$_2^-$)/Chl $a$ in the Fe-limited controls indicate that the high Si : N ratio under the high-CO$_2$ conditions was mainly caused by the decrease in cellular N concentrations of the phytoplankton. Furthermore, the phytoplankton community in the C-600 treatment would be more severely Fe-limited compared to that in the C-380 treatment as described above. This leads the phytoplankton in the C-600 conditions

to have a decrease in Chl $a$ quota (e.g., Sugie et al., 2011); then the difference in the NO$_3^-$ + NO$_2^-$ consumption per unit phytoplankton biomass may be large compared to the measured difference in (NO$_3^-$ + NO$_2^-$)/Chl $a$ values between C-380 and C-600 treatments. Previous studies reported that the C:N ratio of the diatoms was rarely affected by the variations in CO$_2$ levels (Burkhardt et al., 1997, 1999; King et al., 2011; Sun et al., 2011; Sugie and Yoshimura, 2013). This suggests that the C content of the phytoplankton also decreased with increasing CO$_2$ under Fe-limited conditions, leading to an increase in the Si : C ratio in the C-600 treatment. Because N and C assimilations were strongly suppressed in response to the decrease in iron availability (e.g., Raven et al., 1999), we concluded that the high Si : N and Si : C values in high CO$_2$ under Fe-limited conditions were derived from the decrease in iron bioavailability, similarly to the difference observed between the Fe-limited controls and the Fe-added treatments.

The nutrient consumption ratio in the previous field CO$_2$ manipulation studies did not show a significant change in response to the CO$_2$ variations, most of which were conducted with the addition of dissolved inorganic iron (Bering Sea: Martin and Tortell, 2006; North Atlantic: Feng et al., 2009). Therefore, it is important to note that the nutrient drawdown and elemental composition of the particulate matter in the natural phytoplankton communities should be examined under (iron) unamended seawater to forecast the future nutrient biogeochemistry, because iron and nutrient addition potentially alter the community response against the ambient environment. Unfortunately, we have very little data available concerning the effect of CO$_2$ on the Fe-limited natural phytoplankton community. Our other recent studies in the Bering Sea and in the central and western subarctic Pacific regions (conducted in the summer of 2007 and 2008, respectively) reported that no significant change was observed in the Si : N drawdown ratio of the oceanic diatom-dominated
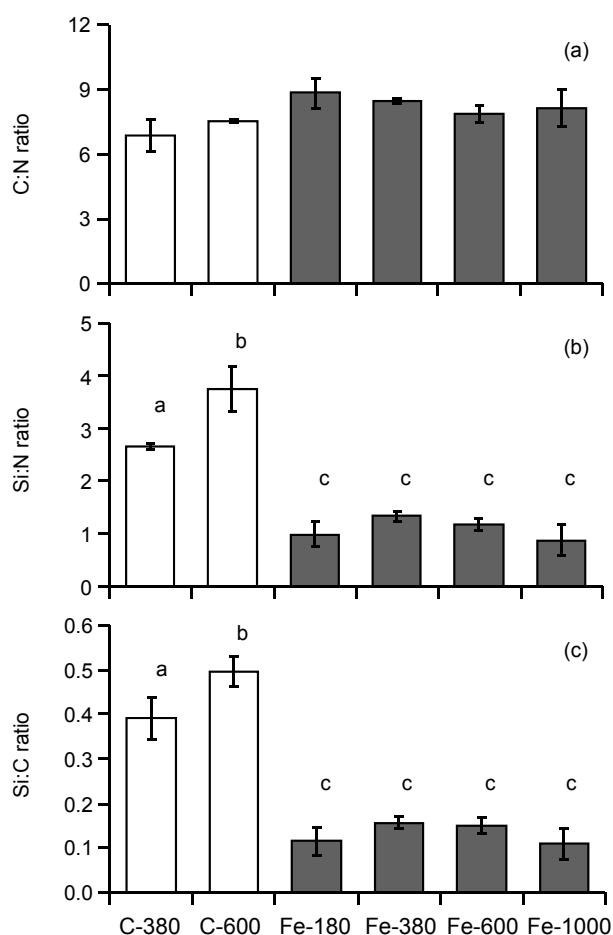
**Fig. 9.** Comparison of particulate **(a)** C : N, **(b)** Si : N and **(c)** Si : C ratios produced during the experiment. Data represent mean ± 1SD of the three bottles. Letters above the bar represent the statistical results of Tukey's B group test.

phytoplankton community (Endo et al., 2013; Yoshimura et al., 2013). As far as we can consider, the factors producing such discrepancies in the Si:N ratio are follows: (i) the difference of the phytoplankton communities; (ii) the non-linear response of the Si : N ratio of the diatoms, which depends on the diatoms' iron nutritional status (Bucciarelli et al., 2010); and/or (iii) difference of the iron-binding ligand, which would differ in the dissociation behavior of bioavailable iron from natural iron-ligand complex in response to the change in CO$_2$ levels (Shi et al., 2010). Further study is apparently needed to clarify the synergistic effects of CO$_2$ and iron on the nutrient stoichiometry of phytoplankton under Fe-limited ecosystems to better understand the ocean biogeochemistry in future high-CO$_2$ oceans.

### 4.3  Implications on nutrient biogeochemistry for the future high-CO$_2$ oceans

The present study is the first demonstration that high CO$_2$ affects nutrient dynamics in Fe-limited phytoplankton communities. The high Si : N and Si : C values under the high-CO$_2$ conditions in the Fe-limited controls probably derived from the further Fe-limitation of coastal diatoms due to the decrease in iron bioavailability. Recent studies indicated that the iron bioavailability and iron distribution will change in future high-CO$_2$ oceans (Mahowald et al., 2009; Millero et al., 2009; Shi et al., 2010); however, there is very limited information available to date on whether the iron availability will increase or not in the future. Our results indicate that iron bioavailability will decrease under future high-CO$_2$ conditions in the oceanic to coastal boundary regions. We suggest that the modulation of the iron bioavailability under the future high-CO$_2$ conditions will be one of the key factors controlling oceanic nutrient biogeochemistry.

The high Si : N and Si : C ratios were derived from the decrease in cellular N and C content of the phytoplankton in the present study. This result indicates that the effect of the biological carbon pump associated with diatoms (Tréguer and Pondaven, 2000) will decrease under high-CO$_2$ conditions. In the PDMPO incubation experiment conducted before nutrient exhaustion, the silicification of a few minor diatom species decreased with increasing CO$_2$ levels, suggesting that the frustule thickness of some diatom species decreased with increasing CO$_2$ levels (Fig. 8). A previous study reported that the dissolution rate of diatom frustule using *Thalassiosira weissflogii* was enhanced due to an increase in CO$_2$ level (Milligan et al., 2004). The Si concentration per unit surface area of the diatom *Pseudo-nitzschia pseudodelicatissima* also decreased with increasing CO$_2$ levels from ∼ 200 to ∼ 750 µatm under various dissolved inorganic iron hydroxide concentrations (Sugie and Yoshimura, 2013). These studies suggest that the silicification of some diatom species can be influenced by the change in ambient CO$_2$ level. There is increasing evidence that the responses of the phytoplankton to high-CO$_2$ conditions are often species- and strain-specific (e.g., Langer et al., 2009; Hutchins et al., 2009). In addition, the low silicon content of diatom cells with low N and C content will be easily remineralized in the upper water column. Because diatom frustule is considered one of the most influential ballast minerals, carrying organic soft tissues to the deep ocean (Passow and De La Rocha, 2006), the fast dissolution of diatomaceous Si with low N and C content causes a further decrease in the effect of biological pump under the future high-CO$_2$ conditions. Therefore, the community composition of diatoms is critical when considering the effect of CO$_2$ on the biogeochemical cycling of nutrients in the surface ocean. The elemental composition and particulate property of each diatom species is an important parameter for predicting the future biogeochemical cycling of nutrients in the oceans.

**Supplementary material related to this article is available online at http://www.biogeosciences.net/10/6309/2013/bg-10-6309-2013-supplement.pdf.**

## References

Arrigo, K. R., Robinson, D. H., Worthen, D. L., Dunbar, R. B., Di-Tullio, G. R., VanWoert, M., and Lizotte, M. P.: Phytoplankton community structure and the drawdown of nutrients and CO$_2$ in the Southern Ocean. Science, 283, 365–367, 1999.

Bucciarelli, E., Pondaven, P., and Sarthou, G.: Effects of an iron-light co-limitation on the elemental composition (Si, C, N) of the marine diatoms Thalassiosira oceanica and Ditylum brightwellii, Biogeosciences, 7, 657–669, doi:10.5194/bg-7-657-2010, 2010.

Buck, K. N. and Bruland, K. W.: The physicochemical speciation of dissolved iron in the Bering Sea, Alaska, Limnol. Oceanogr., 52, 1800–1808, 2007.

Burkhardt, S. and Riebesell, U.: CO$_2$ availability affects elemental composition (C : N : P) of the marine diatom *Skeletonema costatum*, Mar. Ecol. Prog. Ser., 155, 67–76, 1997.

Burkhardt, S., Zondervan, I., and Riebesell, U.: Effect of CO$_2$ concentration on C:N:P ratio in marine phytoplankton: A species comparison, Limnol. Oceanogr., 44, 683–690, 1999.

Caldeira, K. and Wickett, M. E.: Ocean model predictions of chemistry changes from carbon dioxide emissions to the atmosphere and ocean, J. Geophys. Res., 110, C09S04, doi:10.1029/2004JC002671, 2005.

de Baar, H. J. W., Boyd, P. W., Coale, K. H., Landry, M. R., Tsuda, A., Assmy, P., Bakker, D. C. E., Bozec, Y., Barber, R. T., Brzezinski, M. A., Buesseler, K. O., Boyé, M., Croot, P. L., Gervais, F., Gorbunov, Y., Harrison, P. J., Hiscock, W. T., Laan, P., Lancelot, C., Law, C. S., Levasseur, M., Marchetti, A., Millero, F. J., Nishioka, J., Nojiri, Y., van Oijen, T., Riebesell, U., Rijkenberg, M. J. A., Saito, H., Takeda, S., Timmermans, K. R., Veldhuis, M. J. W., Waite A. M., and Wong, C. S.: Synthesis of iron fertilization experiments: From the Iron Age in the Age of Enlightenment, J. Geophys. Res., 110, C09S16, doi:10.1029/2004JC002601, 2005.

Edmond, J. W.: High precision determination of titration alkalinity and total carbon dioxide content of seawater by potentiometric titration, Deep-Sea Res., 17, 737–750, 1970.

Endo, H., Yoshimura, T., Kataoka, T., and Suzuki, K.: Effects of CO$_2$ and iron availability on phytoplankton and eubacterial community compositions in the northwest subarctic Pacific, J. Exp. Mar. Biol. Ecol., 439, 160–175, 2013.

Feng, Y., Hare, C. E., Leblanc, K., Rose, J. M., Zhang, Y., DiTullio, G. R., Lee, P. A., Wilhelm, S. W., Rowe, J. M., Sun, J., Nemcek, N., Gueguen, C., Passow, U., Benner, I., Brown, C., and Hutchins, D. A.: Effects of increased pCO$_2$ and temperature on the North Atlantic spring bloom. I. The phytoplankton community and biogeochemical response, Mar. Ecol. *Prog.* Ser., 388, 13–25, 2009.

Feng, Y., Hare, C. E., Rose, J. M., Handy, S. M., DiTullio, G. R., Lee, P. A., Smith Jr., W. O., Peloquin, J., Tozzi, S., Sun, J., Zhang, Y., Dunbar, R. B., Long, M. C., Sohst, B., Lohan, M., and Hutchins, D. A.: Interactive effects of iron, irradiance and CO$_2$ on Ross Sea phytoplankton, Deep-Sea Res. I, 57, 368–83, 2010.

Finkel, Z. V., Matheson, K. A., Regan, K. S., and Irwin, A. J.: Genotypic and phenotypic variation in diatom silicification under paleo-oceanographic conditions, Geobiology, 8, 433–445, 2010.

Fujishima, Y., Ueda, K., Maruo, M., Nakayama, E., Tokutome, C., Hasegawa, H., Matsui, M., and Sohrin, Y.: Distribution of trace bioelements in the subarctic north Pacific Ocean and the Bering Sea (the R/V Hakuho Maru cruise KH-97-2), J.Oceanogr., 57, 261–273, 2001.

Gorbunov, M. Y. and Falkowski, P. G.: Fluorescence induction and relaxation (FIRe) technique and instrumentation for monitoring photosynthetic processes and primary production in aquatic ecosystems, in: Photosynthesis. Fundamental Aspects to Global Perspectives, edited by: Bruce, D. and van der Est, A., Allen Press, Montreal, 1029–1031, 2004.

Greene, R. M., Geider, R. J., Kolber, Z., and Falkowski, P. G.: Iron-induced changes in light harvesting and photochemical energy conversion processes in eukaryotic algae, Plant Physiol., 100, 565–575, 1992.

Hasle, G. R.: Using the inverted microscope, in: Phytoplankton manual, edited by: Sourina, A., UNESCO, Paris, 191–196, 1978.

Hasle, G. R. and Syvertsen, E. E.: Marine diatoms, in: Identifying Marine Phytoplankton, edited by Tomas, C. R., Academic Press, London, 5–385. 1997.

Hillebrand, H., Durseien, C. D., Kirschtel, D., Pollingher, U., and Zohary, T.: Biovolume calculation for pelagic and benthic microalgae, J. Phycol., 35, 403–424, 1999.

Hopkinson, B. M., Xu, Y., Shi, D., McGinn, P. J., and Morel, F. M. M.: The effect of CO$_2$ on the photosynthetic physiology of phytoplankton in the Gulf of Alaska, Limnol. Oceanogr., 55, 2011–2024, 2010.

Hutchins, D. A., Mulholland, M. R., and Fu, F. X.: Nutrient cycles and marine microbes in a CO$_2$-enriched ocean, Oceanography, 22, 128–145, 2009.

Ichinomiya, M., Gomi, Y., Nakamachi, M., Ota, T., and Kobari, T.: Temporal patterns in silica deposition among siliceous plankton during the spring bloom in the Oyashio region, Deep-Sea Res. II, 57, 1665–1670, 2010.

Johnson, K. S., Chavez, F. P., and Friederich, G. E.: Continental-shelf sediment as a primary source of iron for coastal phytoplankton, Nature, 398, 697–700, 1999.

Karohji, K.: Regional distribution of phytoplankton in the Bering Sea and western and northern subarctic regions of the North Pacific Ocean in summer, in: Biological Oceanography of the Northern North Pacific Ocean, edited by: Takenouchi, A. Y., Idemitsu Shouten, Tokyo, Japan, 99–115, 1972.

Kim, J. M., Lee, K., Shin, K., Kang, J. H., Lee, H. W., Kim, M., Jang, P. G., and Jang, M. C.: The effect of seawater $CO_2$ concentration on growth of a natural phytoplankton assemblage in a controlled mesocosm experiment, Limnol. Oceanogr., 51, 1629–1636, 2006.

King, A. L., Sañudo-Wilhelmy, S. A., Leblanc, K., Hutchins, D. A., and Fu, F.: $CO_2$ and vitamin $B_{12}$ interactions determine bioactive trace metal requirements of a subarctic Pacific diatom, ISME J., 5, 1388–1396, 2011.

Kudo, I.: Change in the uptake and cellular Si:N ratio in diatoms responding to the ambient Si:N ratio and growth phase, Mar. Biol., 143, 39–46, 2003.

Langer, G., Nehrke, G., Probert, I., Ly, J., and Ziveri, P.: Strain-specific responses of Emiliania huxleyi to changing seawater carbonate chemistry, Biogeosciences, 6, 2637–2646, doi:10.5194/bg-6-2637-2009, 2009.

Leblanc, K. and Hutchins, D. A.: New applications of a biogenic silica deposition fluorophore in the study of oceanic diatoms, Limnol. Oceanogr. Methods, 3, 462–476, 2005.

Leblanc, K., Hare, C. E., Boyd, P. W., Bruland, K. W., Sohst, B., Pickmere, S., Lohan, M. C., Buck, K., Ellwood, M., and Hutchins, D. A.: Fe and Zn effects on the Si cycle and diatom community structure in two contrasting high and low-silicate HNLC areas, Deep-Sea Res I, 52, 1842–1864, 2005.

Lewis, E., and Wallance, D. W. R.: Program developed for $CO_2$ system calculations. ORNL/CDIAC-105. Carbon dioxide information analysis center, Oak Ridge National Laboratory, US Department of Energy, Oak Ridge, Tennessee, 1998.

Mahowald, N. M., Engelstaedter, S., Luo, C., Sealy, A., Artaxo, P., Benitez-Nelson, C., Bonnet, S., Chen, Y., Chuang, P. Y., Cohen, D. D., Dulac, F., Herut, B., Johansen, A. M., Kubilay, N., Losno, R., Maenhaut, W., Paytan, A., Prospero, J. M., Shank, L. M., and Siefert, R. L.: Atmospheric iron deposition: global distribution, variability, and human perturbations, Annu. Rev. Mar. Sci., 1, 245–278, 2009.

Marchetti, A. and Harrison, P. J.: Coupling changes in the cell morphology and the elemental (C, N, and Si) composition of the pennate diatom Pseudo-nitzschia due to iron deficiency, Limnol. Oceanogr., 52, 2270–2284, 2007.

Martin, C. L. and Tortell, P. D.: Bicarbonate transport and extra-cellular carbonic anhydrase activity in Bering Sea phytoplankton assemblages: Results from isotope disequilibrium experiments, Limnol. Oceanogr., 51, 2111–2121, 2006.

Menden-Deuer, S. and Lessard, E. J.: Carbon to volume relationships for dinoflagellates, diatoms, and other protist plankton. Limnol. Oceanogr., 45, 569–579, 2000.

Millero, F. J., Woosley, R., DiTrolio, B., and Waters, J.: Effect of ocean acidification on the speciation of metals in seawater, Oceanography, 22, 72–85, 2009.

Milligan, A. J., Varela, D. E., Brzezinski, M. A., and Morel, F. M. M.: Dynamics of silicon metabolism and silicon isotopic discrimination in a marine diatom as a function of $pCO_2$, Limnol. Oceanogr., 49, 322–9, 2004.

Mordy, C. M., Stabeno, P. J., Ladd, C., Zeeman, S., Wisegarver, D. P., Salo, S. A., and Hunt, G. L.: Nutrients and primary production along the eastern Aleutian Island Archipelago, Fish., Oceanogr., 14, 55–76, 2005.

Obata, H., Karatani, H., and Nakayama, E.: Automated determination of iron in seawater by chelating resin concentration

and chemiluminescence detection, Anal. Chem., 65, 1524–1528, 1993.

Onodera, J. and Takahashi, K.: Long-term diatom fluxes in response to oceanographic conditions at Stations AS and SA in the central subarctic Pacific and the Bering Sea, 1990–1998, Deep-Sea Res. I, 56, 189–211, 2009.

Paasche, E.: Silicon content of five marine plankton diatom species measured with a rapid filter method, Limnol. Oceanogr., 25, 474–480, 1980.

Passow, U. and De La Rocha C. L.: Accumulation of mineral ballast on organic aggregates, Glob. Biogeochem. Cy., 20, GB1013, doi:10.1029/2005GB002579, 2006.

Raven, J. A., Evans, M. C. W., and Korb, R. E.: The role of trace metals in photosynthetic electron transport in $O_2$-evolving organisms, Photosynth. Res., 60, 111–149, 1999.

Raven, J., Caldeira, K., Elderfield, H., Hoegh-Guldberg, O., Liss, P., Riebesell, U., Shepherd, J., Turley, C., and Watson, A.: Ocean acidification due to increasing atmospheric carbon dioxide, Royal Society, London, p. 57, 2005.

Redfield, A. C., Ketchum, B. H., and Richards, F. A.: The influence of organisms on the composition of seawater, in: The Sea. Vol. 2, edited by: Hill, M. N., Wiley, New York, 26–77, 1963.

Saito, H. and Tsuda, A.: Influence of light intensity on diatom physiology and nutrient dynamics in the Oyashio region, Prog. Oceanogr., 57, 251–263, 2003.

Saito, M. A., Goepfert, T. J., and Ritt, J. T.: Some thoughts on the concept of colimitation: Three definitions and the importance of bioavailability, Limnol. Oceanogr., 53, 276–90, 2008.

Shi, D., Xu, Y., Hopkinson, B. M., and Morel, F. M. M.: Effect of ocean acidification on iron availability to marine phytoplankton, Science, 327, 676–679, 2010.

Stabeno, P. J., Kachel, D. G., Kachel, N. B., and Sullivan, M. E.: Observations from mooring in the Aleutian Passes: temperature, salinity and transport, Fish. Oceanogr., 39–54, 2005.

Sugie, K. and Yoshimura, T.: Effects of $pCO_2$ and iron on the elemental composition and cell geometry of the marine diatom Pseudo-nitzschia pseudodelicatissima, J. Phycol., 49, 475–488, 2013.

Sugie, K., Kuma, K., Fujita, S., and Ikeda, T.: Increase in Si:N drawdown ratio due to resting spore formation by spring bloom-forming diatoms under Fe- and N-limited conditions in the Oyashio region, J. Exp. Mar. Biol. Ecol., 382, 108–16, 2010a.

Sugie, K., Kuma, K., Fujita, S., Nakayama, Y., and Ikeda, T.: Nutrient and diatom dynamics during late winter and spring in the Oyashio region of the western subarctic Pacific Ocean, Deep-Sea Res. II, 57, 1630–1642, 2010b.

Sugie, K., Kuma, K., Fujita, S., Ushizaka, S., Suzuki, K., and Ikeda, T.: Importance of intracellular Fe pools on growth of marine diatoms by using unialgal cultures and the Oyashio region phytoplankton community during spring, J. Oceanogr., 67, 183–196, 2011.

Sun, J., Hutchins, D. A., Feng, Y., Seubert, E. L., Caron, D. A., and Fu, F. X.: Effects of changing $pCO_2$ and phosphate availability on domoic acid production and physiology of the marine harmful bloom diatom Pseudo-nitzschia multiseries, Limnol. Oceanogr., 56, 829–840, 2011.

Suzuki, R. and Ishimaru, T.: An improved method for the determination of phytoplankton chlorophyll using $N, N$-dimethylformamide, J. Oceanogr. Soc. Jpn., 46, 190–194, 1990.

Suzuki, K., Liu, H., Saino, T., Obata, H., Takano, M., Okamura, K., Sohrin, Y., and Fujishima, Y.: East-west gradients in the photosynthetic potential of phytoplankton and iron concentration in the subarctic Pacific Ocean during early summer, Limnol. Oceanogr., 47, 1581–1594, 2002.

Takahashi, K., Fujitani, N., and Yanada, M.: Long term monitoring of particulate fluxes in the Bering Sea and the central subarctic Pacific Ocean, 1997–2000, Prog. Oceanogr., 55, 95–112, 2002.

Takata, H., Kuma, K., Iwade, S., Isoda, Y., Kuroda, H., and Senjyu, T.: Comparative vertical distributions of iron in the Japan Sea, the Bering Sea, and the western North Pacific Ocean, J. Geophys. Res., 110, C07004, doi:10.1029/2004JC002783, 2005.

Takeda, S.: Influence of iron availability on nutrient consumption ratio of diatoms in oceanic waters, Nature, 393, 774–777, 1998.

Tréguer, P. and Pondaven, P.: Silica control of carbon dioxide, Nature, 406, 358–359, 2000.

Welschmeyer, N. A.: Fluorometric analysis of chlorophyll $a$ in the present of chlorophyll $b$ and pheopigments, Limnol. Oceanogr., 39, 1985–1992, 1994.

Xu, Y., Shi, D., Aristilde, L., and Morel, F. M. M.: The effect of pH on the uptake of zinc and cadmium in marine phytoplankton: Possible role of weak complexes, Limnol. Oceanogr., 57, 293–304, 2012.

Yoshimura, T., Nishioka, J., Suzuki, K., Hattori, H., Kiyosawa, H., and Watanabe, Y. W.: Impacts of elevated CO$_2$ on organic carbon dynamics in nutrient depleted Okhotsk Sea surface waters, J. Exp. Mar. Biol. Ecol., 395, 191–198, 2010.

Yoshimura, T., Suzuki, K., Kiyosawa, T., Ono, T., Hattori, H., Kuma, K., and Nishioka, J.: Impacts of elevated CO$_2$ on particulate and dissolved organic matter production: microcosm experiments using iron-deficient plankton communities in open subarctic waters, J. Oceanogr., 69, 601–618, doi:10.1007/s10872-013-0196-2, 2013.